**Enhancement of Cr(VI) decontamination by irradiated sludge biochar in neutral conditions: Evidence of a possible role of persistent free radicals**

# Enhancement of Cr(VI) decontamination by irradiated sludge biochar in neutral conditions: Evidence of a possible role of persistent free radicals

Zheng Tang [a], Song Zhao [b], Hanzhong Jia [b], Davide Vione [c], Yanming Kang [a], Pin Gao [a,d,*]

[a] College of Environmental Science and Engineering, Donghua University, Shanghai 201620, China

[b] College of Resources and Environment, Northwest A & F University, Yangling 712100, Shaanxi, China

[c] Dipartimento di Chimica, Università di Torino, Via Pietro Giuria 5, 10125 Torino, Italy

[d] National-Regional Joint Engineering Research Center for Soil Pollution Control and Remediation in South China, Guangdong Key Laboratory of Integrated Agro-environmental Pollution Control and Management, Guangdong Institute of Eco-environmental Science & Technology, Guangdong Academy of Sciences, Guangzhou 510650, China

* Corresponding author

E-mail: pingao@dhu.edu.cn (Pin Gao)

Postal address: 2999 North Renmin Road, Songjiang District, Shanghai 201620, China

Phone: +86-21-67792535. Fax: +86-21-67792522.

## Abstract

The effect of photo-irradiation on the removal of Cr(VI) by sludge biochar in neutral conditions is here investigated. The results indicate that photo-irradiation can significantly enhance the removal of aqueous Cr(VI) by sludge biochar. The apparent removal rate constants under ultraviolet (0.61 $h^{-1}$) and visible-light (0.27 $h^{-1}$) irradiation are more than 5 and 2 times higher, respectively, than that in the dark (0.11 $h^{-1}$). Cr(VI) reduction plays a predominant role in Cr removal, accounting respectively for 72% of total removal (dark), 72% (visible light irradiation), and 92% (ultraviolet irradiation). The abundance of persistent free radicals (PFRs) in biochar (produced hydrothermally at a temperature of 220°C, a reaction time of 2 h, and a solid weight ratio of 40%w) can reach up to $4.72\times10^{16}$ spins/g, and their EPR signal intensity remains almost unchanged within 720 min in the dark. Ultraviolet irradiation may promote PFRs production in biochar, and PFRs (especially the oxygen-centered ones) act as electron donors to transform Cr(VI) into Cr(III), thereby contributing to Cr(VI) reduction. Our findings shed new light on the role of irradiation in enhancing the removal of Cr(VI) by sludge biochar under neutral conditions, which could be an interesting technique in the field of environmental remediation.



*Keywords*: sludge biochar; persistent free radicals; photo-irradiation; Cr(VI) reduction; adsorption

## 1. Introduction

Persistent free radicals (PFRs) are widely detected in different environmental matrices (Chen et al., 2019; Jia et al., 2017; Yang et al., 2017; Zhao et al., 2019), and have even been identified as a new class of contaminants of emerging concern (Vejerano et al., 2018). Compared with the traditional oxidative free radicals, PFRs have typical features of strong durability, low reactivity, and potential persistent toxicity (Odinga et al., 2020). A number of studies have reported that PFRs have adverse effects on biological systems via the production of reactive oxygen species (ROS) (Dellinger et al., 2001; Zhang et al., 2019a). Therefore, researches on PFRs in the environment have increased rapidly in recent years.

PFRs are commonly produced by electron transfer between organic substances and/or derivatives and transition metals during heat conversion processes, such as biomass-based pyrolysis and hydrothermal conversion (biochar) (Gao et al., 2018; Pan et al., 2019). Abundant PFRs are detected in the pyrolytic and hydrothermal carbon-rich solids, which are generally called biochar. Previous investigations have shown that PFRs in biochar could trigger neurotoxicity in *Caenorhabditis elegans* (Lieke et al., 2018) and inhibit seed germination and growth (Liao et al., 2014). Moreover, biochar-related PFRs were also reported to act by catalytic activation in the generation of ROS, such as •OH, $^1O_2$, $O_2^-$, $H_2O_2$, $SO_4^{\bullet-}$, and $O_3$ (Khachatryan et al., 2011), facilitating the degradation and transformation of organic and inorganic contaminants (Qin et al., 2018; Yang et al., 2017; Zhong et al., 2019). For example, Qin et al. (2018) comprehensively reviewed the PFRs-mediated catalytic oxidation/reduction of refractory organics in carbon-based materials. Ruan et al. (2019) also reviewed the degradation of pollutants by the ROS produced by biochar PFRs. Compared to organic compounds, fewer studies have been carried out on the transformation of heavy metals mediated by PFRs associated to biochar. Zhong et al. (2019) recently observed the oxidation of trivalent arsenic (As(III)) by •OH and $H_2O_2$, generated from activation of $O_2$ by biochar-PFRs. Similarly, Dong et al. (2014) reported that semiquinone radicals in dissolved organic matter (DOM) derived by biochar played a key role in As(III) oxidation. Many additional studies have also investigated the redox processes of hexavalent chromium (Cr(VI)) mediated by biochar-PFRs. Cr(VI) has severe toxicity to human health, and it is known to be 100-fold more toxic than trivalent chromium (Cr(III)) (Saha et al., 2011). Therefore, reduction

of Cr(VI) to Cr(III) is commonly considered as a useful remediation method. A study by Xu et al. (2019) has shown that oxygen-centered PFRs in peanut-shell biochar acted as electron shuttles in the presence of lactate to enhance Cr(VI) reduction under acidic conditions (i.e., pH 2 or 4). Zhong et al. (2018) reported that incorporation of magnetite ($Fe_3O_4$) onto biochar promoted the generation of carbon-centered PFRs, serving as electron donors for Cr(VI) reduction. Zhu et al. (2020) also found enhanced Cr(VI) transformation, due to the presence of PFRs as electron donors in nitrogen-doped biochar. However, these studies are always performed in acidic conditions (i.e., pH 2-4) because it is commonly believed that low pH values enhance Cr(VI) removal, owing to the electrostatic attraction between the positively charged biochar surface and the negative Cr(VI) species (i.e., $Cr_2O_7^{2-}$ and $HCrO_4^-$) (Kotaś and Stasicka, 2000). By contrast, Zhao et al. (2018) observed that corn straw biochar was able to remove Cr(VI) at pH ~ 7, and recognized the possible role of semiquinone-type PFRs as the electron donors for Cr(VI) reduction. Nevertheless, the key role of PFRs in biochar in the transformation of Cr(VI) in neutral conditions is still unclear.

Sludge is the by-product of sewage treatment, and it needs proper handling due to the harmful chemicals and pathogens it contains (Ivanová et al., 2018). In China, the production of sludge is growing fast due to the increasing amount of sewage wastewater. It has been reported that approximately 30 million tons of wet sludge is generated annually (Zhang et al., 2017). In the past few decades the proper recycling of sludge for the recovery of resource and energy has been a key topic worldwide, and a number of methods have been proposed (Kacprzak et al., 2017; Teoh and Li, 2020). Among these, conversion of sludge into valuable biochar is regarded as an attractive route, due to the potential application of biochar as soil amendment and its favorable performance in pollutant removal (Qian et al., 2020). A recent study found that PFRs were generated during hydrothermal carbonization of sewage sludge (Zhu et al., 2019). Similar results were found by Chen et al. (2020), who reported that generation of carbon-centered PFRs was induced in the hydrothermal conversion of waste sludge into biochar. Several researches have also shown that PFRs generated in sludge biochar facilitated degradation of organic contaminants through the generation of ROS (Qin et al., 2017; Wang and Wang, 2019). Moreover, it has been reported that light could induce PFRs formation in the environment (Jia et al., 2019; Shi et al., 2020), which may then influence the environmental behavior of contaminants (Fang et al., 2017; Inasaridze et al., 2017; Yi et al.,

2019). Chen et al. (2017) observed that biomass-based hydrochar (produced hydrothermally) generated more $H_2O_2$ and •OH than pyrochar (produced by pyrolysis) under daylight irradiation, due to the abundance of PFRs in hydrochar that enhanced sulfadimidine degradation. However, studies on the sludge biochar-mediated transformation of heavy metals are limited, and the exact role of PFRs is still uncertain.

In this study, we prepared biochar from sewage sludge and investigated its performance for the adsorption and reduction of Cr(VI), in the dark and under photo-irradiation conditions. The aims of this work are (1) to investigate the removal performance of Cr(VI) by sludge biochar in neutral conditions in the dark, as well as under ultraviolet and visible-light irradiation; (2) to explore whether biochar PFRs are able to reduce Cr(VI), and (3) to highlight the different pathways involved in Cr(VI) removal by sludge biochar under different light conditions.

## 2. Experimental section

### 2.1 Materials and chemicals

Chemicals including potassium bromide (KBr), potassium dichromate ($K_2Cr_2O_7$), sulfuric acid ($H_2SO_4$), phosphoric acid ($H_3PO_4$), diphenylcarbazide, acetone, potassium permanganate ($K_2MnO_4$), sodium nitrite ($NaNO_2$), and urea were all purchased from Sinopharm Chemical Reagent Co., Ltd (Shanghai, China), and used without further purification unless specified. DPPH (2,2-diphenyl-1-picrylhydrazyl), used as a stable free-radical standard in this study, was obtained from Sigma-Aldrich.

### 2.2 Hydrothermal preparation of sludge biochar

Waste sludge used in this study was collected from the secondary settling tank of Songjiang sewage treatment plant (STP) in Shanghai. Raw sludge was first precipitated overnight and the settled solids were freeze-dried with an LGJ-10E freeze dryer (Sihuan, Beijing, China). The dried pellets were ground into powder and screened through a 40-mesh sieve (the mesh aperture was 0.425 mm). Visual impurities such as plant fragments and grains of sand in sludge were eliminated with tweezers prior to the hydrothermal process. To prepare sludge biochar, 30 g dried sludge powder was transferred into a 100-mL PPL-lined stainless steel

autoclave with 75 mL deionized water, and heated at 220°C for 2 h in an oven. During hydrothermal carbonization, the sludge aqueous solution was magnetically stirred at a speed of 800 rpm. After reaction, the reactor was allowed to room temperature naturally and the resulting solids were washed with ethanol and deionized water for several times. The final products were freeze-dried and stored in amber bottles for subsequent characterization and experiments.

### 2.3 Batch experiments for Cr(VI) adsorption and reduction

Batch experiments were performed to investigate adsorption and reduction of Cr(VI) by sludge biochar. A stock solution of Cr(VI) (1.0 g/L) was prepared by dissolving a certain amount of $K_2Cr_2O_7$ in deionized water, and the Cr(VI) working solution was prepared by diluting the above stock solution. Then, 60 mL of the Cr(VI) working solution (2.0 mg/L) was mixed with 50 mg of biochar in each 100-mL quartz tube, ensuring that the final concentration of the biochar was about 0.8 g/L. To ensure that pH conditions were representative of the environment, the solution pH in this study was adjusted to 7.0 with diluted sulfuric acid and sodium hydroxide solutions. A blank experiment with biochar without Cr(VI), and a control with Cr(VI) without biochar were performed in parallel for comparison. In order to determine the effect of photo-irradiation on the adsorption and reduction of Cr(VI) by biochar, visible-light was used following the same procedures and irradiating under a 350 W Xenon lamp with a cutoff filter ($\lambda > 420$ nm) (Ji et al., 2020), while ultraviolet radiation was produced by a deuterium arc lamp (190 nm $< \lambda <$ 400 nm). The biochar-water mixture was magnetically stirred at 150 rpm at room temperature, kept constant with a water cooling system. Control tests in the dark were also performed. At each preset time, the mixture solution was collected and centrifuged. The supernatant was filtered through 0.22 μm syringe filters, and the contents of total Cr and of Cr(VI) were quantified using a spectrophotometric method.

### 2.4 Analytical methods

The intensity of PFRs in biochar was measured by an electron paramagnetic resonance spectrometer (EPR, EMXmicro-6/1/P/L, Bruker, Karlsruhe Germany) at room temperature. Briefly, approximately 50 mg of biochar were transferred into a high-purity quartz EPR

micro-tube having an inner-diameter of 4 mm, which was subsequently sealed with grease at one tip prior to measurement. The EPR operating parameters such as microwave frequency and power, and central field are referred to our previously reported studies (Gao et al., 2018; Jia et al., 2016). The PFRs concentration is calculated by comparison with standards, based on the quantitative theory. Fourier transform infrared (FTIR) spectra were used to investigate the changes of functional groups in biochar before and after Cr(VI) transformation, and were obtained with a Tensor 27 FTIR spectrometer (Bruker, Germany). Briefly, approximately 3 mg of biochar were compressed with 300 mg of spectrally-pure KBr. Then, the obtained tablet was placed on the FTIR instrument and scanned in the wavenumber range of 4000 - 400 $cm^{-1}$, with a resolution of 4 $cm^{-1}$.

Concentrations of total Cr and of Cr(VI) in the solutions under investigation were determined using a diphenylcarbazide-based spectrophotometric method at 540 nm (GB 7466-87 and GB 7467-87, Standards of China), with a UV-5200PC UV-vis spectrophotometer (METASH, China). The Cr(III) concentration in solution was then calculated by subtracting Cr(VI) from the total Cr. The total Cr adsorbed by biochar was obtained as the difference between the initial and the measured amounts of total Cr in solution. The species occurring at the biochar surface, including Cr(VI) and Cr(III) were measured by X-ray photoelectron spectroscopy (XPS, Escalab 250Xi, Thermo Scientific, USA). XPS Peak 4.1 software was used to analyze the XPS core layer spectra. The metal contents in raw sewage sludge and biochar samples were measured using an inductive coupled plasma emission spectrometer (ICP-OES, Prodigy, Leeman Labs, USA).

### 2.5 Statistical analysis

Averages and standard deviations of data were calculated by Microsoft Excel 2016. Statistical analyses were performed with SPSS 19.0 (SPSS Inc., Chicago, IL, USA), using the significance threshold $p < 0.05$. All plots were generated with the OriginPro 9.0 software (OriginLab Corporation, USA).

## 3. Results and discussion

### 3.1 Characterization of the sludge biochar

PFRs have commonly been found in hydrothermally converted biomass, including sewage sludge (Zhu et al., 2019). As shown in Fig. 1(a), a singlet EPR signal is detected in biochar and the PFRs concentration can reach up to $4.72\times10^{16}$ spins/g. In contrast, the EPR signal in raw sludge is relatively weaker (Fig. 1a), which is possibly ascribed to the low content of metal oxides such as iron and aluminum oxides (Fig. 1b). The g-factor value of biochar is calculated at 2.0034, indicating coexistence of oxygen- and carbon-centered radicals (Jia et al., 2017).

During the hydrothermal process, the main components of sewage sludge (i.e., cellulose and protein) would be hydrolyzed and cleaved to generate PFRs by the catalytic effect of subcritical water. FTIR spectra (Fig. 1c) of raw sludge and biochar clearly indicate that the peak at around 1240 $cm^{-1}$ associated with phenolic O-H disappears, while the peak at around 1050 $cm^{-1}$ representing phenolic C-O is enhanced, implying that phenolic O-H is probably transformed into phenoxyl radicals. The peak at around 1440 $cm^{-1}$ corresponding to C=C bonds in the aromatic and heterocyclic rings (He et al., 2013) is enhanced, suggesting possible formation of aromatic radicals due to aromatization (Fang et al., 2014). Overall, there is consistency between FTIR and EPR results.

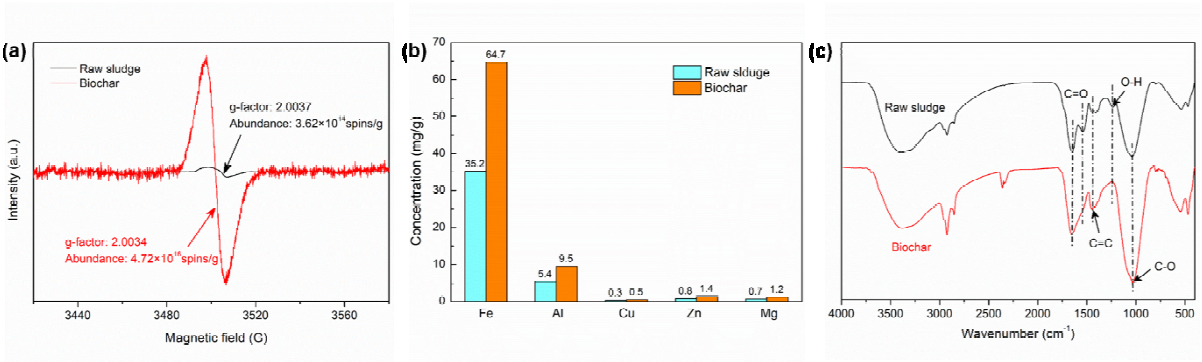


**Fig. 1.** Characterization of raw sludge and biochar. (a) EPR signals; (b) contents of heavy metals; (c) FTIR spectra.

### 3.2 Cr(VI) reduction by sludge biochar during the adsorption process

Figure 2 shows variations in the concentrations of Cr(VI) and Cr(III) in solution, induced by sludge biochar during the adsorption process at pH 7. As indicated, the aqueous Cr(VI)

concentration gradually decreased from 2.0 to 0.92 mg/L within 720 min in the dark (Fig. 2a), while aqueous Cr(III) was initially absent and its content correspondingly increased up to 0.30 mg/L (Fig. 2b). This result indicates that sludge biochar is able to reductively transform Cr(VI) into Cr(III), and also that Cr(VI) and/or Cr(III) is adsorbed by biochar, as indicated by the decrease in total Cr. Mass balance calculations suggest an adsorption capacity for total Cr of 0.94 $mg_{Cr}/g_{biochar}$, approximately accounting for 39% of the initial quantity of total Cr.

There are studies reporting that oxygen-containing functional groups in carbon-based materials, such as hydroxyl and carboxyl contribute greatly to Cr(VI) adsorption via complexation, ion exchange, and electrostatic interaction (Huang et al., 2016; Ma et al., 2019; Yang et al., 2019; Zhao et al., 2018). In this work, however, we found no apparent difference in the surface functional groups of biochar before and after Cr(VI) adsorption in the dark (Fig. 3), suggesting that the direct interaction of Cr(VI) with biochar is not the key factor controlling Cr(VI) adsorption.

It is commonly recognized that Cr(VI) adsorption is pH-dependent and that acidic conditions favor Cr(VI) adsorption (Fan et al., 2019), because the oxygen-containing functional groups on the solid surface can be protonated to form positively charged groups, which can interact with the negatively charged Cr species such as $Cr_2O_7^{2-}$ and $HCrO_4^-$ via electrostatic attraction (Huang et al., 2016; Zhong et al., 2018). However, Zhao et al. (2018) observed that corn-straw biochars had quite high adsorption capacity of Cr(VI) even at pH 7 with an initial Cr(VI) concentration < 5 mg/L (i.e., 1 and 2 mg/L), although this was a little lower compared to the adsorption capacity at pH 3. Likewise, we also find here that about 54% of Cr(VI) was removed by biochar at pH 7 with an initial Cr(VI) concentration of 2 mg/L, confirming a favorable removal of Cr(VI) by biochar in neutral conditions. The occurrence of Cr(III) in solution (Fig. 2b) suggests that the reduction of Cr(VI) into Cr(III) may play an important role in the removal of Cr(VI) during the adsorption process.

Contrary to Cr(VI), Cr(III) seems easier to be stabilized in the presence of biochar (Chen et al., 2015; Yu et al., 2018). In order to examine the Cr species adsorbed onto biochar, we used the XPS technique and the results are shown in Fig. 4. Reasonably, both Cr(VI) and Cr(III) were detected. The binding energy values of 589.4 eV and 580.0 eV are associated with Cr(VI), while 577.1 eV and 586.9 eV are assigned to Cr(III). The proportions of Cr(VI) and Cr(III) are 39.0% and 61.0%, respectively (Fig. 4a).

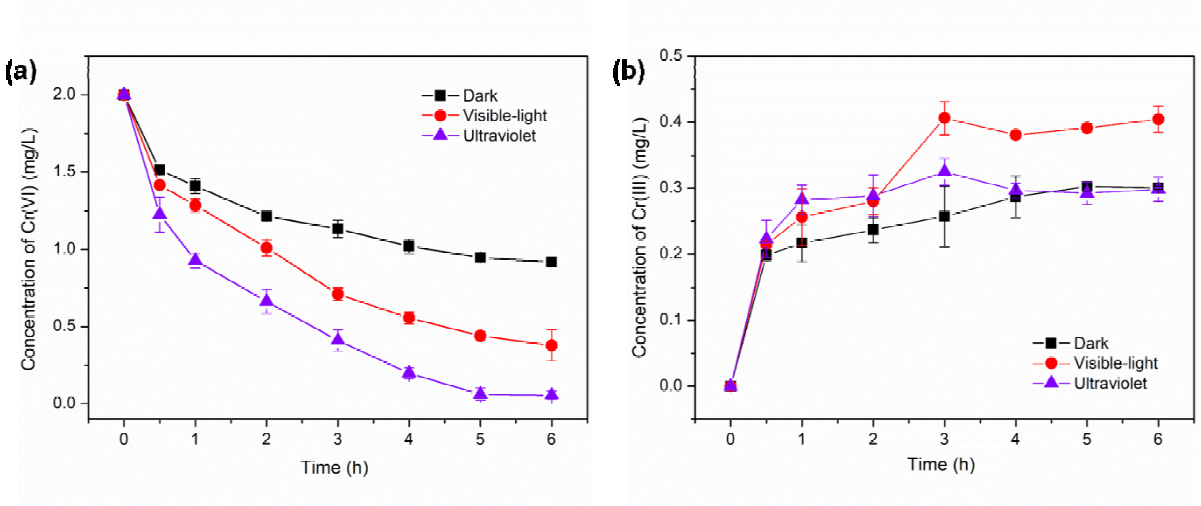


**Fig. 2.** Variations in concentrations of (a) Cr(VI) and (b) Cr(III) during the adsorption process by sludge biochar at pH 7 in the dark, as well as under visible-light and ultraviolet irradiation.

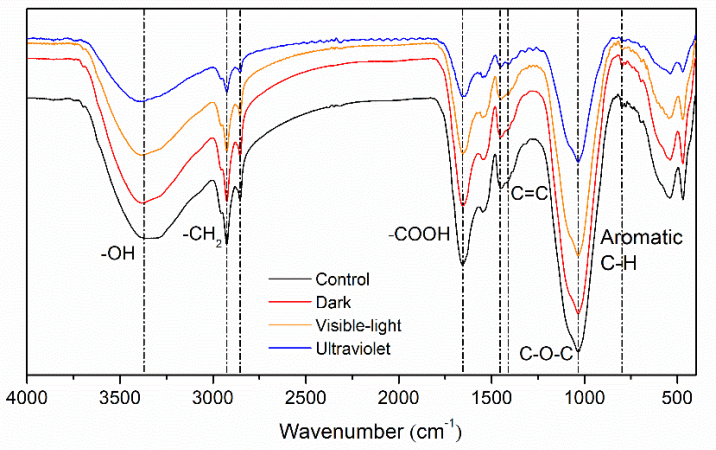


**Fig. 3.** FTIR spectra of biochar before and after Cr(VI) removal at pH 7 in the dark, and under visible-light and ultraviolet irradiation. "Control" represents the biochar in solution without Cr(VI) in the dark.

On this basis, calculations suggest that the contribution of Cr(VI) reduction to the total Cr removal was 72%, of which 44% (i.e., 72×0.61 %, where 0.61 is the fraction of Cr(III) occurring on the surface of biochar) would be accounted for by Cr(III) adsorbed on biochar, and 28% to Cr(III) remaining in solution. This finding suggests that reduction played a predominant role in the removal of Cr(VI) by biochar adsorption. It is very interesting to report this significant reduction capacity of Cr(VI) by sludge biochar at pH 7 in the dark, i.e., far from the optimal pH conditions for the reduction of Cr(VI) to Cr(III), which occurs best in acidic solution.

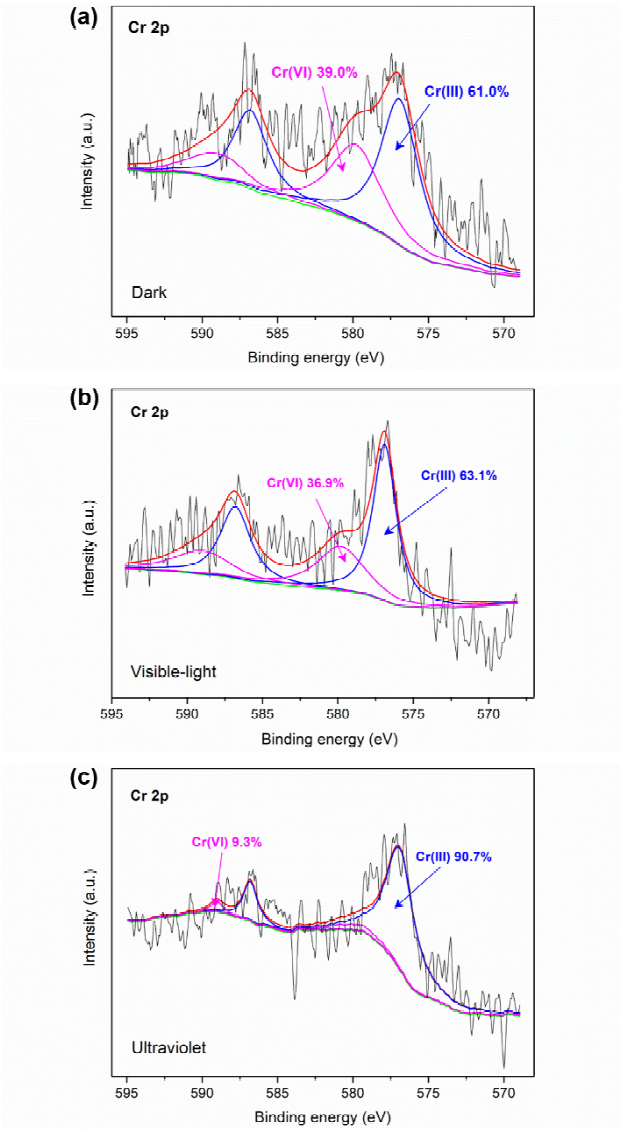


**Fig. 4.** XPS analysis of Cr species in biochar after Cr(VI) removal. (a) Dark condition; (b) visible-light irradiation; (c) ultraviolet irradiation.

Actually, increasing the solution pH towards ~neutral conditions should slow down the reduction process (Choppala et al., 2016). A possible explanation for our finding is that biochar PFRs (Fig. 1a) can act as electron donors for the reduction of Cr(VI) to Cr(III), which will be dealt with later. Similar results were reported by Xu et al. (2019), who showed that biochar produced from peanut shell acted as electron donor for Cr(VI) reduction. We could thus speculate that biochar could reduce Cr(VI) to Cr(III), and that a fraction of the latter could be adsorbed on the biochar surface and possibly precipitate there, due to the formation of $Cr(OH)_3$ and/or $Cr_2O_3$ at relatively high pH (Chen et al., 2015; Yang et al., 2019; Yu et al.,

2018), while the rest of Cr(III) remained in solution. Precipitation of Cr(III) on the biochar surface, rather than complexation of Cr by oxygen-containing groups, could explain why the corresponding FTIR signals in biochar were not modified significantly by the addition of Cr salts (Fig. 3). Additionally, about 28% of the Cr adsorbed by biochar was in the form of Cr(VI). This is possibly attributed to the occurrence of ion exchange ,or other interaction between Cr(VI) and other metals contained in biochar (Fig. 1b) (Fan et al., 2019).

### 3.3 Effect of photo-irradiation on Cr(VI) removal

Photo-irradiation has been commonly used to promote electron transfer in biochar-based materials, to enhance the degradation of organic compounds through formation of ROS (Fang et al., 2017; Fu et al., 2016; Ye et al., 2019). Ward et al. (2014) have previously reported that sunlight can decompose the light-absorbing condensed aromatics contained in particulate biochar suspended in water, possibly affecting electron transfer (Wang et al., 2010). Therefore, we carried out ultraviolet and visible-light irradiation tests to study the removal of Cr(VI) in neutral conditions. As shown in Fig. 2(a), the removal of Cr(VI) was significantly ($p < 0.05$) enhanced by ultraviolet irradiation compared to the dark experiment. The aqueous Cr(VI) concentration under irradiation decreased from 2.0 to 0.06 mg/L within 720 min, obtaining an excellent removal rate of up to 97%. At the same time, interestingly, the aqueous Cr(III) concentration increased to 0.30 mg/L, which is very close to the value found in the dark (Fig. 2b). Calculations suggest that 82.5% of the total Cr was adsorbed by biochar with an adsorption capacity of 1.98 mg/g, which is twice higher than that observed in the dark (0.94 mg/g). This indicates that ultraviolet irradiation greatly enhanced Cr adsorption by biochar. In addition to adsorption, reduction of Cr(VI) to Cr(III) also occurred. XPS spectra show that Cr(VI) and Cr(III) in biochar accounted, respectively, for 9.3% and 90.7% of the total surface Cr (Fig. 4c), thereby suggesting that reduction was the dominant pathway of Cr(VI) removal from the solution, and that ultraviolet irradiation enhanced the reduction of Cr(VI).

Visible-light irradiation could also enhance Cr(VI) removal compared to dark experiments, although the improvement was a little lower than under ultraviolet irradiation (Fig. 2a). The aqueous Cr(VI) concentration was decreased from 2.0 to 0.38 mg/L within 720 min, with a total removal rate of 81.0%. At the same time, the aqueous Cr(III) concentration increased to 0.40 mg/L, which is a little higher than that in the dark and under ultraviolet

irradiation (Fig. 2b). Adsorbed Cr was 61.0% of the total added Cr, with an adsorption capacity by biochar of 1.46 mg/g that is about 55% higher than that in the dark. The XPS results showed the occurrence of both Cr(VI) and Cr(III), with respective proportions of 37% and 63% (Fig. 4b) that are very similar to those observed in the dark (Fig. 4a). On this basis, one gets that Cr(VI) reduction would account for 72% of total Cr removal. The apparent first-order kinetics has been widely used to evaluate adsorption and oxidation/reduction processes (Gao et al., 2017; Wang et al., 2019). As shown in Fig. 5, it is evident that photo-irradiation can greatly increase the $k_{app}$ values of Cr(VI) removal by biochar: the $k_{app}$ values under visible-light (0.27 $h^{-1}$) and ultraviolet (0.61 $h^{-1}$) irradiation are, respectively, 2 and 5 times higher than in the dark (0.11 $h^{-1}$). This finding further illustrates that Cr(VI) removal by biochar is significantly enhanced by photo-irradiation, especially under ultraviolet.

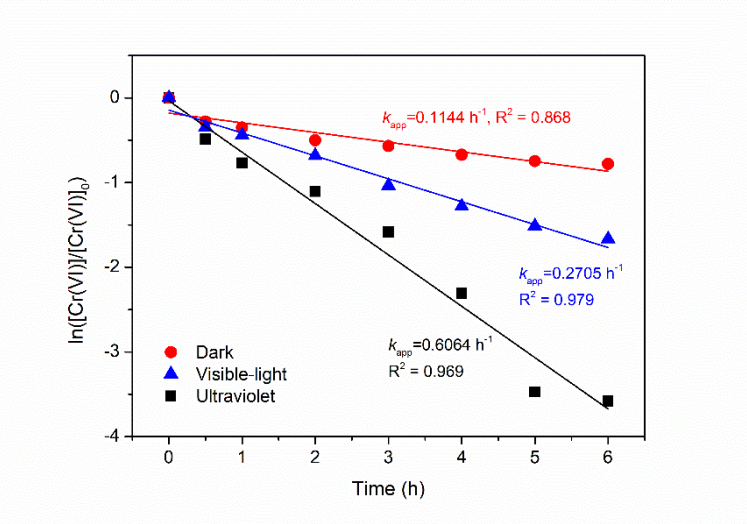


**Fig. 5.** Linear plotting of ln([Cr(VI)]/[Cr(VI)$_0$]) versus time ($t$) based on the apparent first-order kinetic model ln([Cr(VI)]/[Cr(VI)$_0$]) = – $k_{app} \times t$, where [Cr(VI)]$_0$ stands for the initial Cr(VI) concentration (mg/L), [Cr(VI)] represents the Cr(VI) concentration at time $t$ in solution (mg/L), and $k_{app}$ is the apparent rate constant ($h^{-1}$).

### 3.4 Involvement of PFRs in the removal of Cr(VI)

The above results clearly show a predominant contribution of the reduction mechanism to the total removal of Cr(VI), which is most likely ascribed to reductive moieties in biochar due to the absence of other electron donors in solution. Although the oxygen-containing functional

groups such as –OH and C–O–C can serve as electron-donors, their reduction abilities are relatively weak in neutral and alkaline conditions (Ma et al., 2019). Therefore, we hypothesize that the favorable reduction of Cr(VI) is probably associated with other stronger electron donors, such as PFRs detected in biochar (Fig. 1a), which have been previously reported to mediate reduction processes (Xu et al., 2019; Zhao et al., 2018; Zhang et al., 2019b). As indicated in Fig. 6(a), the abundance of PFRs in biochar is relatively stable within 6 h in the dark, with a small decline of 5.1% (compare the “Biochar" signal in Fig. 1(a) with the "Control" signal in Fig. 6(a)).

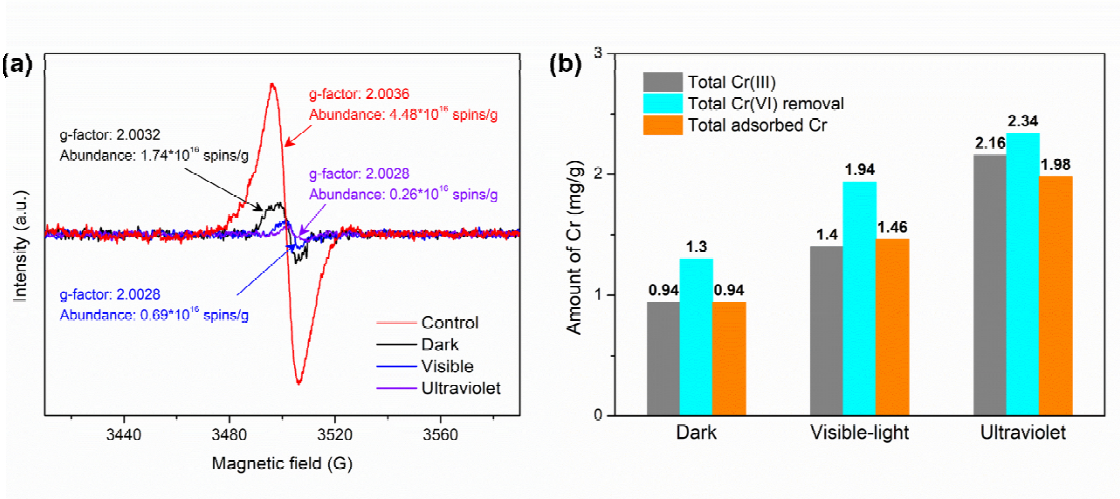


**Fig. 6.** (a) EPR signals detected in biochar before and after Cr(VI) removal, at pH 7 in the dark and under visible-light and ultraviolet irradiation. Control: no added Cr(VI), 6h in the dark; Dark: signal taken 6h after Cr(VI) addition in the dark; Visible & Ultraviolet: : signal taken 6h after Cr(VI) addition, under the specified irradiation conditions. (b) Quantities of the total adsorbed Cr, the removed Cr(VI), and the produced Cr(III) during the adsorption process by biochar.

In contrast, a significant ($p < 0.05$) decrease of the EPR signal from $4.5\times10^{16}$ to $1.7\times10^{16}$ spins/g was induced by the Cr(VI) adsorption process, suggesting that PFRs in biochar are consumed in the presence of Cr(VI), which may have a certain effect on Cr(VI) removal. At the same time as the decrease of the EPR signal, the g-factor values decreased from 2.0036 to 2.0032, which suggests a certain relative enrichment in carbon-centered radicals. A likely explanation for this finding is that oxygen-containing radicals may act as electron donors for

Cr(VI) reduction, as already hypothesized by Zhao et al. (2018).

Irradiation conditions had an additional, evident effect on the abundances of PFRs in biochar, resulting in significant ($p < 0.05$) reductions of the EPR signals down to $0.69\times10^{16}$ and $0.26\times10^{16}$ spins/g under visible-light and ultraviolet irradiation, respectively. This results is consistent with the above results of Cr(VI) reduction to Cr(III), and it suggests that PFRs may play an important role in the reductive removal of Cr(VI) under irradiation conditions. Moreover, the g-factor values under irradiation both decreased down to 2.0028, which further suggests an even higher percentage of carbon-centered radicals in biochar after Cr adsorption, compared to the dark conditions. Again, this is compatible with a selective involvement of oxygen-containing radicals (e.g., phenoxyls) into Cr(VI) reduction.

Based on the overall results reported so far, we can conclude that the effective removal of Cr(VI) by biochar, especially under ultraviolet irradiation stems from a combination of adsorption and reduction, and that the latter process likely involves PFRs to a possibly significant extent. In the dark, Cr(VI) reduction is likely followed by precipitation of $Cr(OH)_3$ and/or $Cr_2O_3$ that would be favored under neutral conditions, thereby explaining the detection of Cr(III) on the biochar surface by XPS measurements (Fig. 4). At the same time, FTIR measurements of the biochar samples after contact with Cr(VI) in the dark showed no changes in the signals of oxygen-containing functional groups (i.e., –OH, –COOH, and C–O–C) (Fig. 3), which would exclude significant interaction between these groups and adsorbed Cr.

Reduction of Cr(VI) to Cr(III) is enhanced under (especially) ultraviolet irradiation, and these conditions are also well known to favor the occurrence of PFRs on the surface of biochar. Moreover, FTIR measurements suggest that the oxygen-containing functional groups are significantly modified after ultraviolet irradiation in the presence of Cr(VI) (Fig. 3), which is compatible with a role they may play in the interaction with adsorbed Cr species. Therefore, in addition to Cr(VI) reduction and $Cr(OH)_3$ / $Cr_2O_3$ precipitation, Cr removal under irradiation conditions might also proceed through a significant involvement of some function groups on the surface of biochar, which might take part to, e.g., the adsorption process. To sum up, the possible processes involved in Cr(VI) removal by biochar are presented in Fig. 7.

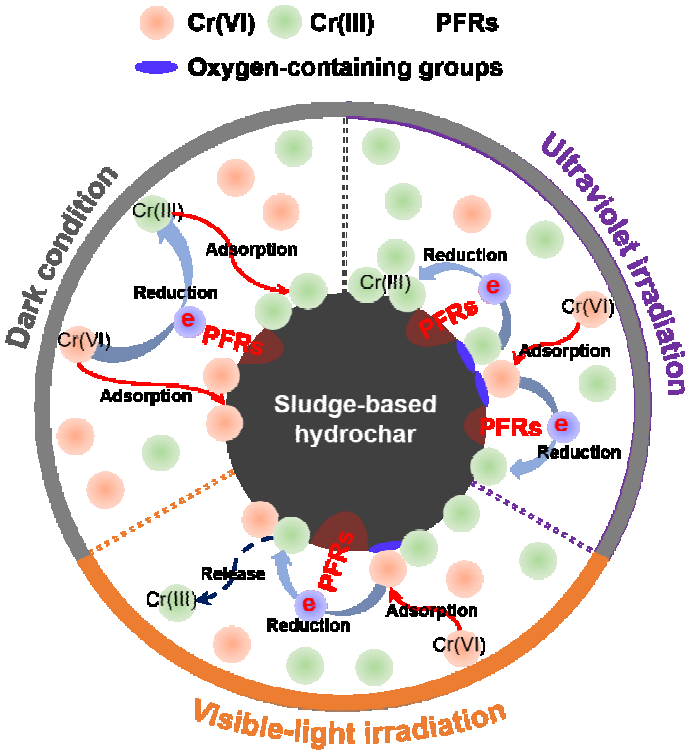


**Fig. 7.** Possible mechanisms of Cr(VI) removal in neutral solution by sludge biochar, in the dark and under visible-light and ultraviolet irradiation. Circles in orange and green represent Cr(VI) and Cr(III), respectively, while ovals in red and blue represent PFRs and oxygen-containing functional groups, respectively.

## 4. Conclusions

Sludge biochar obtained by hydrothermal carbonization was used to investigate the removal process of Cr(VI) under different light conditions at neutral pH. The results showed that, compared to dark conditions, ultraviolet and visible-light irradiation can both significantly enhance the removal of aqueous Cr(VI) by biochar. Reduction of Cr(VI) to Cr(III), followed or accompanied by Cr(III) precipitation on biochar, and by Cr adsorption on the biochar surface is shown here to play a key role in the process. There is also evidence that PFRs occurring in hydrothermally produced biochar, or additionally generated by ultraviolet irradiation may take part to the reduction process. A predominant role among PFRs is likely played by oxygen-centered radicals. This work provides insight into the removal processes of Cr(VI) at neutral pH using sludge biochar under photo-irradiation, which may have potential application in the field of environmental remediation.

**Acknowledgements**

This work was financially supported by the Guangxi Innovation Drive Development Fund (grant number AA17204076); the GDAS' Project of Science and Technology Development (grant number 2020GDASYL-20200102014); and the National Key R&D Program of China (grant number 2019YFD1100502).

**References**


Chen, N., Huang, Y., Hou, X., Ai, Z., Zhang, L., 2017. Photochemistry of hydrochar: reactive oxygen species generation and sulfadimidine degradation. Environ. Sci. Technol. 51, 11278-11287.

Chen, C., Liu, G., An, Q., Lin, L., Shang, Y., Wan, C., 2020. From wasted sludge to valuable biochar by low temperature hydrothermal carbonization treatment: insight into the surface characteristics. J. Clean. Prod. 263,121600

Chen, Q., Sun, H., Mu, Z., Wang, Y., Li, Y., Zhang, L., Wang, M., Zhang, Z., 2019. Characteristics of environmentally persistent free radicals in PM2.5: concentrations, species and sources in Xi'an, Northwestern China. Environ. Pollut. 247, 18-26.

Chen, T., Zhou, Z., Xu, S., Wang, H., Lu, W., 2015. Adsorption behavior comparison of trivalent and hexavalent chromium on biochar derived from municipal sludge. Bioresource Technol. 190, 388-394.

Choppala, G., Bolan, N., Kunhikrishnan, A., Bush, R., 2016. Differential effect of biochar upon reduction-induced mobility and bioavailability of arsenate and chromate. Chemosphere 144, 374-381.

Dellinger, B., Pryor, W.A., Cueto, R., Squadrito, G.L., Hegde, V., Deutsch, W. A., 2001. Role of free radicals in the toxicity of airborne fine particulate matter. Chem. Res. Toxicol. 14, 1371-1377.

Dong, X., Ma, L.Q., Gress, J., Harris, W., Li, Y., 2014. Enhanced Cr(VI) reduction and As(III) oxidation in ice phase: important role of dissolved organic matter from biochar. J. Hazard. Mater. 267, 62-70.

Fan, Z., Zhang, Q., Gao, B., Li, M., Liu, C., Qiu, Y., 2019. Removal of hexavalent chromium by biochar supported nZVI composite: batch and fixed-bed column evaluations, mechanisms, and secondary contamination prevention. Chemosphere 217, 85-94.

Fang, G., Gao, J., Liu, C., Dionysiou, D.D., Wang, Y., Zhou, D., 2014. Key role of persistent free radicals in hydrogen peroxide activation by biochar: implications to organic contaminant degradation. Environ. Sci. Technol. 48, 1902-1910.

Fang, G., Liu, C., Wang, Y., Dionysiou, D.D., Zhou, D., 2017. Photogeneration of reactive oxygen species from biochar suspension for diethyl phthalate degradation. Appl. Catal.

B. - Environ. 214, 34-45.

Fu, H., Liu, H., Mao, J., Chu, W., Li, Q., Alvarez, P.J., Qu, X., Zhu, D., 2016. Photochemistry of dissolved black carbon released from biochar: reactive oxygen species generation and phototransformation. Environ. Sci. Technol. 50, 1218-1226.

Gao, P., Gu, C., Wei, X., Li, X., Chen, H., Jia, H., Liu, Z., Xue, G., Ma, C., 2017. The role of zero valent iron on the fate of tetracycline resistance genes and class 1 integrons during thermophilic anaerobic co-digestion of waste sludge and kitchen waste. Water Res. 111, 92-99.

Gao, P., Yao, D., Qian, Y., Zhong, S., Zhang, L., Xue, G., Jia, H., 2018. Factors controlling the formation of persistent free radicals in hydrochar during hydrothermal conversion of rice straw. Environ. Chem. Lett. 16, 1463-1468.

He, C., Giannis, A., Wang, J.Y., 2013. Conversion of sewage sludge to clean solid fuel using hydrothermal carbonization: hydrochar fuel characteristics and combustion behavior. Appl. Energ. 111, 257-266.

Huang, X., Liu, Y., Liu, S., Tan, X., Ding, Y., Zeng, G., Zhou, Y., Zhang, M., Wang, S., Zheng, B., 2016. Effective removal of Cr(VI) using β-cyclodextrin-chitosan modified biochars with adsorption/reduction bifuctional roles. RSC Adv. 6, 94-104.

Inasaridze, L.N., Shames, A.I., Martynov, I.V., Li, B., Mumyatov, A.V., Susarova, D.K., Katz, E.A., Troshin, P.A., 2017. Light-induced generation of free radicals by fullerene derivatives: an important degradation pathway in organic photovoltaics? J. Mater. Chem. A. 5, 8044-8050.

Ivanova, L., Mackulak, T., Grabic, R., Golovko, O., Koba, O., Stanova, A.V., Szabova, P., Grencikova, A., Bodik, I., 2018. Pharmaceuticals and illicit drugs - a new threat to the application of sewage sludge in agriculture. Sci. Total Environ. 634, 606-615.

Ji, L., Liu, B., Qian, Y., Yang, Q., Gao, P., 2020. Enhanced visible-light-induced photocatalytic disinfection of Escherichia coli by ternary $Bi_2WO_6/TiO_2$/reduced graphene oxide composite materials: insight into the underlying mechanism. Adv. Powder Technol. 31, 128-138.

Jia, H., Nulaji, G., Gao, H., Wang, F., Zhu, Y., Wang, C., 2016. Formation and stabilization of environmentally persistent free radicals induced by the interaction of anthracene with Fe(III)-modified clays. Environ. Sci. Technol. 50, 6310-6319.

Jia, H., Zhao, S., Nulaji, G., Tao, K., Wang, F., Sharma, V.K., Wang, C., 2017. Environmentally persistent free radicals in soils of past coking sites: distribution and stabilization. Environ. Sci. Technol. 51, 6000-6008.

Jia, H., Zhao, S., Shi, Y., Zhu, K., Gao, P., Zhu, L., 2019. Mechanisms for light-driven evolution of environmentally persistent free radicals and photolytic degradation of PAHs on Fe(III)-montmorillonite surface. J. Hazard. Mater. 362, 92-98.

Kacprzak, M., Neczaj, E., Fijalkowski, K., Grobelak, A., Grosser, A., Worwag, M., Rorat, A., Brattebo, H., Almas, A., Singh, B.R., 2017. Sewage sludge disposal strategies for sustainable development. Environ. Res. 156, 39-46.

Khachatryan, L., Vejerano, E., Lomnicki, S., Dellinger, B., 2011. Environmentally persistent free radicals (EPFRs). 1. Generation of reactive oxygen species in aqueous solutions. Environ. Sci. Technol. 45, 8559-8566.

Kotaś, J., Stasicka, Z., 2000. Chromium occurrence in the environment and methods of its speciation. Environ. Pollut. 107, 263-283.

Li, Q., Ding, W., Yong, Y., Zeng, X., Gao, Y., 2016. Effects of ultraviolet modification on physicochemical property and adsorption performance of biochar. Nanosci. Nanotechnol. Lett. 8, 978-984.

Liao, S., Pan, B., Li, H., Zhang, D., Xing, B., 2014. Detecting free radicals in biochars and determining their ability to inhibit the germination and growth of corn, wheat and rice seedlings. Environ. Sci. Technol. 48, 8581-8587.

Lieke, T., Zhang, X., Steinberg, C.E.W., Pan, B., 2018. Overlooked risks of biochars: persistent free radicals trigger neurotoxicity in *Caenorhabditis elegans*. Environ. Sci. Technol. 52, 7981-7987.

Ma, H., Yang, J., Gao, X., Liu, Z., Liu, X., Xu, Z., 2019. Removal of chromium (VI) from water by porous carbon derived from corn straw: influencing factors, regeneration and mechanism. J. Hazard. Mater. 369, 550-560.

Odinga, E.S., Waigi, M.G., Gudda, F.O., Wang, J., Yang, B., Hu, X., Li, S., Gao, Y., 2020. Occurrence, formation, environmental fate and risks of environmentally persistent free radicals in biochars. Environ. Int. 134, 105172.

Pan, B., Li, H., Lang, D., Xing, B., 2019. Environmentally persistent free radicals: Occurrence, formation mechanisms and implications. Environ. Pollut. 248, 320-331.

Peng, Z., Zhao, H., Lyu, H., Wang, L., Huang, H., Nan, Q., Tang, J., 2018. UV modification of biochar for enhanced hexavalent chromium removal from aqueous solution. Environ. Sci. Pollut. Res. 25, 10808-10819.

Qian, T., Lu, D., Soh, Y.N.A., Webster, R.D., Zhou, Y., 2020. Biotransformation of phosphorus in enhanced biological phosphorus removal sludge biochar. Water Res. 169, 115255.

Qin, Y., Li, G., Gao, Y., Zhang, L., Ok, Y.S., An, T., 2018. Persistent free radicals in carbon-based materials on transformation of refractory organic contaminants (ROCs) in water: a critical review. Water Res. 137, 130-143.

Qin, Y., Zhang, L., An, T., 2017. Hydrothermal carbon-mediated fenton-like reaction mechanism in the degradation of alachlor: direct electron transfer from hydrothermal carbon to Fe(III). ACS Appl. Mater. Inter. 9, 17115-17124.

Ruan, X., Sun, Y., Du, W., Tang, Y., Liu, Q., Zhang, Z., Doherty, W., Frost, R.L., Qian, G., Tsang, D.C.W., 2019. Formation, characteristics, and applications of environmentally persistent free radicals in biochars: a review. Bioresource Technol. 281, 457-468.

Saha, R., Nandi, R., Saha B., 2011. Sources and toxicity of hexavalent chromium. J. Coord. Chem. 64, 1782-1806.

Shi, Y., Dai, Y., Liu, Z., Nie, X., Zhao, S., Zhang, C., Jia, H., 2020. Light-induced variation in environmentally persistent free radicals and the generation of reactive radical species in humic substances. Front. Env. Sci. Eng. 14, 1-10.

Teoh, S.K., Li, L.Y., 2020. Feasibility of alternative sewage sludge treatment methods from a lifecycle assessment (LCA) perspective. J. Clean. Prod. 247, 119495.

Vejerano, E.P., Rao, G., Khachatryan, L., Cormier, S.A., Lomnicki, S., 2018. Environmentally persistent free radicals: insights on a new class of pollutants. Environ. Sci. Technol. 52, 2468-2481.

Wang, X.S., Chen, L.F., Li, F.Y., Chen, K.L., Wan, W.Y., Tang, Y.J., 2010. Removal of Cr (VI) with wheat-residue derived black carbon: reaction mechanism and adsorption performance. J. Hazard. Mater. 175, 816-822.

Wang, H., Guo, W., Yin, R., Du, J., Wu, Q., Luo, H., Liu, B., Sseguya, F., Ren, N., 2019. Biochar-induced Fe(III) reduction for persulfate activation in sulfamethoxazole degradation: Insight into the electron transfer, radical oxidation and degradation

pathways. Chem. Eng. J. 362, 561-569.

Wang, S., Wang, J., 2019. Activation of peroxymonosulfate by sludge-derived biochar for the degradation of triclosan in water and wastewater. Chem. Eng. J. 356, 350-358.

Ward, C.P., Sleighter, R.L., Hatcher, P.G., Cory, R.M., 2014. Insights into the complete and partial photooxidation of black carbon in surface waters. Environ. Sci. – Proc. Imp. 16, 721-731.

Xu, X., Huang, H., Zhang, Y., Xu, Z., Cao, X., 2019. Biochar as both electron donor and electron shuttle for the reduction transformation of Cr(VI) during its sorption. Environ. Pollut. 244, 423-430.

Xu, Z., Xu, X., Zhang, Y., Yu, Y., Cao, X., 2020. Pyrolysis-temperature depended electron donating and mediating mechanisms of biochar for Cr(VI) reduction. J. Hazard. Mater. 388, 121794.

Yang, L., Liu, G., Zheng, M., Jin, R., Zhu, Q., Zhao, Y., Wu, X., Xu, Y., 2017. Highly elevated levels and particle-size distributions of environmentally persistent free radicals in haze-associated atmosphere. Environ. Sci. Technol. 51, 7936-7944.

Yang, X., Wan, Y., Zheng, Y., He, F., Yu, Z., Huang, J., Wang, H., Ok, Y.S., Jiang, Y., Gao, B., 2019. Surface functional groups of carbon-based adsorbents and their roles in the removal of heavy metals from aqueous solutions: a critical review. Chem. Eng. J. 366, 608-621.

Ye, S., Yan, M., Tan, X., Liang, J., Zeng, G., Wu, H., Song, B., Zhou, C., Yang, Y., Wang, H., 2019. Facile assembled biochar-based nanocomposite with improved graphitization for efficient photocatalytic activity driven by visible light. Appl. Catal. B. - Environ. 250, 78-88.

Yi, P., Chen, Q., Li, H., Lang, D., Zhao, Q., Pan, B., Xing, B., 2019. A comparative study on the formation of environmentally persistent free radicals (EPFRs) on hematite and goethite: contribution of various catechol degradation byproducts. Environ. Sci. Technol. 53, 13713-13719.

Yu, J., Jiang, C., Guan, Q., Ning, P., Gu, J., Chen, Q., Zhang, J., Miao, R., 2018. Enhanced removal of Cr(VI) from aqueous solution by supported ZnO nanoparticles on biochar derived from waste water hyacinth. Chemosphere 195, 632-640.

Zhang, Y., Guo, X., Si, X., Yang, R., Zhou, J., Quan, X., 2019a. Environmentally persistent

free radical generation on contaminated soil and their potential biotoxicity to luminous bacteria. Sci. Total. Environ. 687, 348-354.

Zhang, Q., Hu, J., Lee, D.J., Chang, Y., Lee, Y.J., 2017. Sludge treatment: current research trends. Bioresource Technol. 243, 1159-1172.

Zhang, K., Sun, P., Zhang, Y., 2019b. Decontamination of Cr(VI) facilitated formation of persistent free radicals on rice husk derived biochar. Front. Env. Sci. Eng. 13, 22.

Zhao, S., Gao, P., Miao, D., Wu, L., Qian, Y., Chen, S., Sharma, V.K., Jia, H., 2019. Formation and evolution of solvent-extracted and nonextractable environmentally persistent free radicals in fly ash of municipal solid waste incinerators. Environ. Sci. Technol. 53, 10120-10130.

Zhao, N., Yin, Z., Liu, F., Zhang, M., Lv, Y., Hao, Z., Pan, G., Zhang, J., 2018. Environmentally persistent free radicals mediated removal of Cr(VI) from highly saline water by corn straw biochars. Bioresource Technol. 260, 294-301.

Zhong, D., Jiang, Y., Zhao, Z., Wang, L., Chen, J., Ren, S., Liu, Z., Zhang, Y., Tsang, D.C.W., Crittenden, J.C., 2019. pH dependence of arsenic oxidation by rice-husk-derived biochar: roles of redox-active moieties. Environ. Sci. Technol. 53, 9034-9044.

Zhong, D., Zhang, Y., Wang, L., Chen, J., Jiang, Y., Tsang, D.C.W., Zhao, Z., Ren, S., Liu, Z., Crittenden, J.C., 2018. Mechanistic insights into adsorption and reduction of hexavalent chromium from water using magnetic biochar composite: key roles of $Fe_3O_4$ and persistent free radicals. Environ. Pollut. 243, 1302-1309.

Zhu, S., Huang, X., Yang, X., Peng, P., Li, Z., Jin, C., 2020. Enhanced Transformation of Cr(VI) by Heterocyclic-N within Nitrogen-doped biochar: impact of surface modulatory persistent free radicals (PFRs). Environ. Sci. Technol. 54, 8123-8132.

Zhu, Y., Wei, J., Liu, Y., Liu, X., Li, J., Zhang, J., 2019. Assessing the effect on the generation of environmentally persistent free radicals in hydrothermal carbonization of sewage sludge. Sci. Rep. 9, 17092.